Acousto-optic imaging using quantum memories in cryogenic rare earth ion doped crystals

Luke R. Taylor, Alexander Doronin, Igor Meglinski, Jevon J. Longdell

Luke R. Taylor, Alexander Doronin, Igor Meglinski, Jevon J. Longdell, "Acousto-optic imaging using quantum memories in cryogenic rare earth ion doped crystals," Proc. SPIE 8943, Photons Plus Ultrasound: Imaging and Sensing 2014, 89431D (3 March 2014); doi: 10.1117/12.2038775

SPIE.

Event: SPIE BiOS, 2014, San Francisco, California, United States

Acousto-optic imaging using quantum memories in cryogenic rare earth ion doped crystals

Luke R. Taylor*[a], Alexander Doronin[a], Igor Meglinski[a], Jevon J. Longdell[a]
[a]University of Otago, Department of Physics, 730 Cumberland St, Dunedin 9016, New Zealand

ABSTRACT

The interaction of ultrasound and light in biological tissues results in a small amount of the scattered light being shifted relative to the carrier frequency (typically 1 part in 10^8). We have developed an inherently efficient and low noise quantum memory based technique to selectively absorb these 'ultrasound tagged' photons in a pair of atomic frequency combs, and recover them delayed in time as a photon echo. In this manner we have demonstrated record ultrasound-modulated sideband-to-carrier discrimination (49dB). Further, we confirm that the technique is compatible with highly scattering samples, and present initial acoustic pulse tracking measurements. This strongly suggests the suitability of the technique for biological tissue imaging.

Keywords: optical detection of ultrasound, ultrasound-modulated optical tomography, acousto-optic imaging, quantum memory, atomic frequency comb, cryogenic rare-earth ions.

1. INTRODUCTION

Ultrasound modulated optical tomography (UMOT) is the detection of ultrasound in a medium using an optical source, and the reconstruction of the detected signal into a volume (3-D) image. It has applications for the imaging of biological soft tissues and early cancer detection.

Unfortunately light is highly scattered in such tissues, and the penetration depth for highly sensitive, all-optical imaging techniques is limited. In contrast, acoustic imaging is less sensitive but does not suffer from scattering in tissue. We combine the advantages of both acoustic and optical imaging in this acousto-optic UMOT technique.

As a narrowband optical source is scattered through a medium, it will undergo sideband modulation in the presence of ultrasound (see Figure 1). This occurs via a combination of scattering from moving particles and changes in refractive index over the scattered path due to the acoustic (compression) wave. Our premise is that the resulting sidebands can be detected optically, and an image reconstructed based on the known timing of the (focused) ultrasound pulse (or rather, train of pulses).

However, the relative frequency shift is typically only 1 part in 10^8 (ratio of the ultrasound to optical frequencies), and the net modulation depth is small (limited interaction or common volume, combined with low intensities and further losses). Extremely sensitive filters are thus required for the detection of these signals. Given the high optical scattering, interferometers[1] and optical cavities[2] are not suited; high etendue is required. Photorefractive (PR) techniques[3-5] have been developed to overcome this issue, but remain too slow (10-100ms)[6, 7] for the imaging of living biological samples (the decorrelation time in biological tissues is typically 0.1ms[8]).

Spectral holeburning as a means for creating high-contrast filters in cryogenically cooled rare earth ion doped crystals has recently been of interest. This can be achieved particularly effectively at around 606nm in Pr^{3+}:Y_2SiO_5, due to the long spectral hole lifetime. A 14dB difference in transmission between carrier and a single sideband[9], and an order of magnitude improvement in etendue over PR crystals[10], have been demonstrated. The dispersive properties of spectral holes have also been used for sensitive detection of ultrasound[11], as well as slow light to further suppress input pulse to background noise[12].

*luke.taylor@otago.ac.nz

Photons Plus Ultrasound: Imaging and Sensing 2014, edited by Alexander A. Oraevsky, Lihong V. Wang,
Proc. of SPIE Vol. 8943, 89431D · © 2014 SPIE · CCC code: 1605-7422/14/$18 · doi: 10.1117/12.2038775

We have chosen to use quantum memory based techniques for the optical detection of ultrasound, given that effective quantum memories display high efficiency and very low noise- both properties also being necessary for the sensitive detection of ultrasound. Using the atomic frequency comb (AFC) as our quantum memory of choice, we have demonstrated record optical sideband to carrier discrimination (49dB)[13].

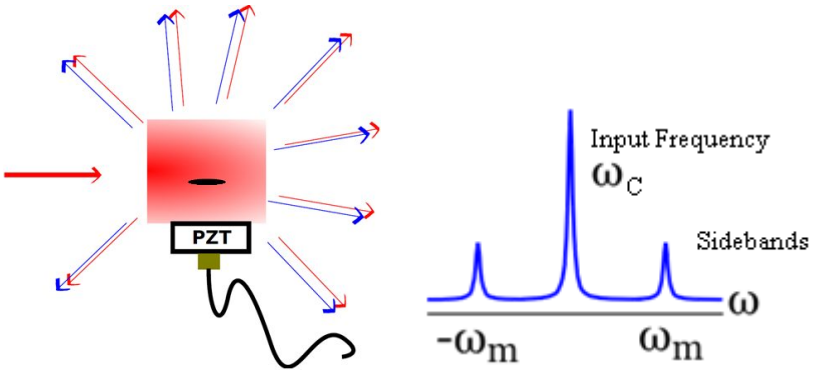

Figure 1. Schematic of the ultrasound modulated sideband generation. An acoustic pulse (black oval) is generated by a transducer, and is focused through a scattering medium (e.g., biological tissue sample). A pulse of light with carrier frequency ω_C is also incident on the sample. Interactions within the common volume (sampled by both light and ultrasound) result in some of the scattered light being shifted in frequency by $\pm\omega_M$, we call these 'ultrasound tagged photons'.

As described in earlier work[13] we achieve this by writing a pair of (absorptive) AFCs on either side of a (transmissive) window, tuned to the ultrasound sideband modulation and carrier frequencies respectively. Figure 2 shows a typical spectral readout sweep over the AFC pair; this is acquired by slowly scanning a low intensity beam in frequency across the combs.

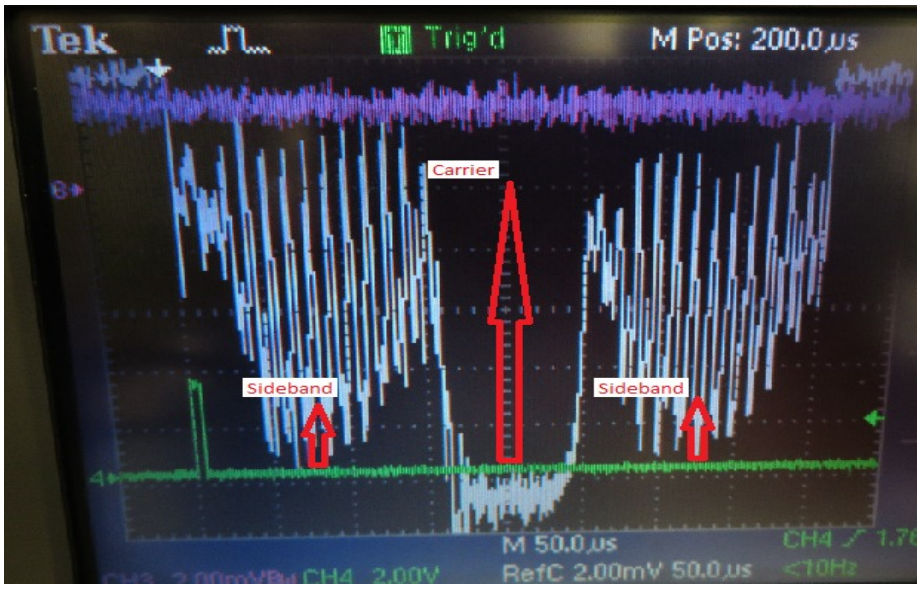

Figure 2. The white trace illustrates the atomic frequency comb (AFC) pair, centered about a swept-out spectral transmission window. This central window is at the carrier frequency. Approximate relative positions of the carrier and sideband frequencies are indicated. The ultrasonically tagged photons are absorbed in the comb, to be retrieved at a later time as a photon echo as defined by the comb parameters.

The light absorbed in the AFCs is retrieved later in time as a photon echo, as defined by the comb parameters (tooth separation ~150kHz, finesse ~2, optical depth $\alpha L \sim 2$, echo retrieval delay ~6.67μs). Admittedly, not all the tagged photons are delayed into this echo, but only those photons shifted in frequency (having interacted with the acoustic pulse) and also interacting with the AFC, are delayed. To this we attribute our exceptional sideband to carrier discrimination. We note that the technique relies solely on optical pumping, and does not require additional fields.

Much of our previous work was aimed at establishing high sideband to carrier discrimination, and relied upon balanced heterodyne detection of the signal mixed with a local oscillator. We did extend the work to the direct detection of photon echoes stored in the AFCs from a highly scattered beam (achieving a detector limited 29dB discrimination) yet all modulated sidebands were artificially generated using an electro-optic modulator (EOM).

In this work, we focus on applying the described technique to the detection of truly acoustically generated optical sidebands in a representatively scattering soft medium, and present initial 1-D imaging results.

2. EXPERIMENTAL METHOD

Figure 3 shows the set-up used for the experiments described here. We aim to optically detect ultrasound modulated sidebands generated from acousto-optic interactions within a defined common volume encompassing both input ultrasound (acoustic) and optical (probe) pulses.

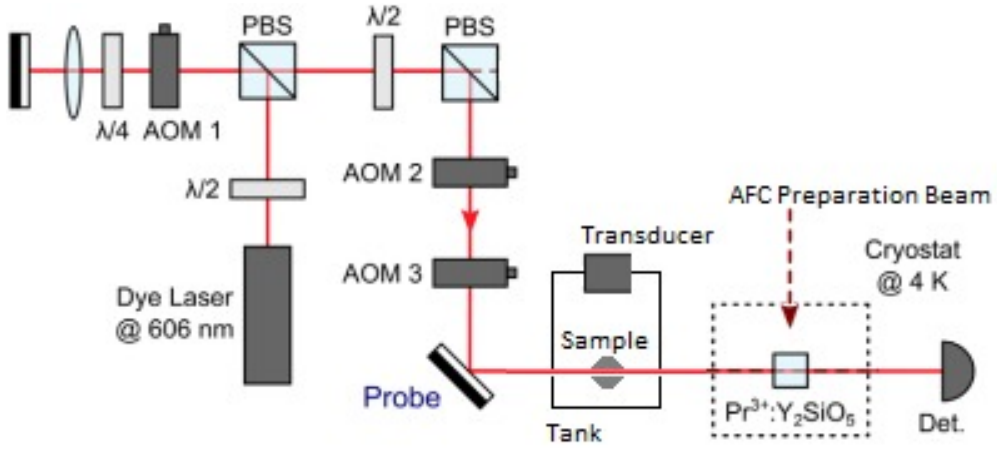

Figure 3. Schematic of the experimental setup used for tracking the transducer-generated acoustic pulse through the scattering sample. AOM: acousto-optic modulators for frequency agility and time gating. λ/2, λ4: half and quarter waveplates for polarization control. The probe beam is in solid red, and the beam used for writing the AFC pair in dashed red. The $Pr^{3+}:Y_2SiO_5$ sample used for the spectral filter is cooled in a home-built condensing He cryostat. A gated PMT is used for signal detection.

The optical source is a Coherent 699 dye laser, with additional in-house frequency stabilization (ca. 5kHz linewidth). The AFC pair and central transparency window are prepared solely via optical pumping in a cryogenically cooled 5x5x5 mm^3 $Pr^{3+}:Y_2SiO_5$ sample, as described in more detail elsewhere[13]. This requires careful frequency control (achieved via the double-pass AOM1) and time gating (using AOM2 and AOM3). A fourth AOM (not shown, in the AFC preparation beam) acts as a switch and completes the setup for the AFC preparation beam.

The probe beam (optical input pulse) does not pass through this fourth AOM but instead is incident on a clear Plexiglas tank containing the sample to be imaged, as illustrated schematically. Typical samples are firm gels made up of agar (at around 1.5% by weight in distilled water), with additions of intralipid (at 20% solution) in varying percentages, to adjust scattering coefficient. Absorbing elements (e.g., inclusions of agar gel set with black ink) can also easily be added.

A large collecting lens is used to focus the scattered (and frequency shifted) light through the AFC pair written in the Pr^{3+} ions within the cryostat. Another lens collects and collimates the light at the output of the cryostat before sending it to a gated photomultiplier tube (PMT) for detection. We have added a spatial aperture within the cryostat to ensure that only light passing through the filter reaches the detector.

The ultrasound pulse (typically 1μs in duration, providing ca. 1.5mm resolution along the acoustic propagation axis) is generated using a 1MHz ultrasonic immersion transducer from Olympus. This is acoustically coupled to the sample (phantom) using distilled water, and focused to just under 1mm diameter in the plane perpendicular to the direction of propagation.

Timing of the entire experiment is done using a multichannel radio frequency PulseBlaster radio processor from SpinCore Technologies. Given the sidebands are only generated from within the common acousto-optic volume, we are able to spatially reconstruct the signal if the precise timing of the acoustic pulses is known. A well-defined series of acoustic pulses (and their echoes retrieved from the AFCs) should thus enable 1-D imaging on a particular column.

A typical experiment is made up as follows. First we optically prepare the $Pr^{3+}:Y_2SiO_5$ sample to a repeatable initial state. Then we write the AFC pair optically, and sweep out the central transmission window using the AFC preparation beam as illustrated in Figure 2 and described in[13]. Finally we apply a series of acoustic and optical pulses with adjustable (or swept) relative timing delays and detect the respective photon echoes, to provide a series of signals along the acoustic axis: a 1-D image through the sample. We expect to achieve planar and volume (2-D and 3-D) mapping simply through translation of the sample.

3. RESULTS AND DISCUSSION

Figure 4 shows a photograph of the setup, with the Plexiglas tank, agar gel phantom and transducer. A train of focussed acoustic pulses (blue) and the probe pulse path (red) have been overlaid schematically. Distilled water serves to impedance match the transducer and acoustic couple the compression wave to the sample. The input light pulse is highly scattered in the agar gel, and the collecting lens can be seen behind the tank.

Figure 4. Photograph of the setup including the acoustic transducer and agar phantom contained within the Plexiglas tank. Schematically overlaid are the train of (focused) acoustic pulses (in blue), and the input optical path (in red). The large collecting lens can be seen behind the sample; the black background is the wall of the cryostat's outer vacuum chamber.

A typical spatial distribution of the scattered light sent through the cryostat (and AFC filter) is illustrated in the following Figure 5. The somewhat square edges are due to the shape of the light shield placed in the cryostat, spatially blocking light that does not also pass through the (spectral) filter.

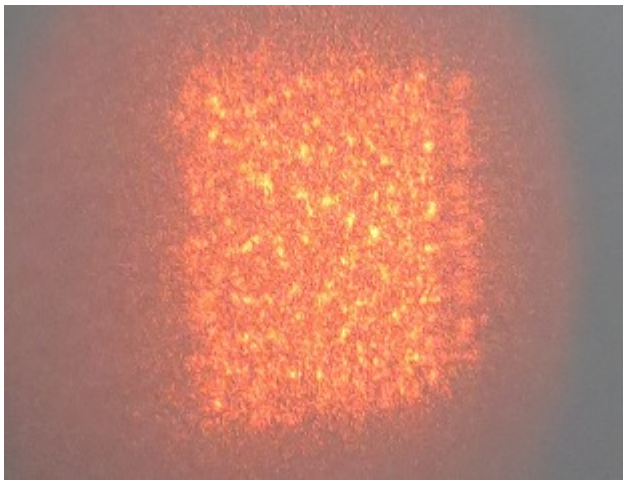

Figure 5. Image (projected on to a white paper screen) illustrating the spatial distribution of light passing through the light shield, AFC based filter and cryostat. This light is then sent on to the gated photomultiplier for echo detection.

As described, we prepare the initial state for the filter and write the AFC pair and window. We then send in a series of acoustic and optical pulses, with incremental delays in relative timing corresponding to common acousto-optic volumes deeper and deeper into the phantom (further along the acoustic propagation axis). The gated photomultiplier tube is triggered for each pulse and only opened when the echo is expected. The signal is acquired on an oscilloscope and averaged over a number of repetitions. A typical trace is shown in Figure 6.

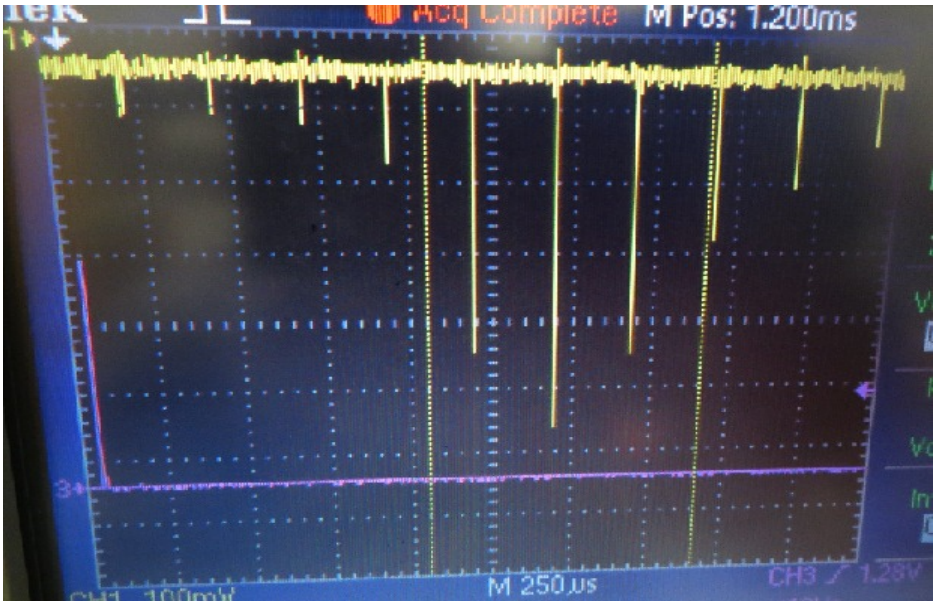

Figure 6. Oscilloscope trace showing the pulse (photon echo) sequence obtained from a series of acoustic pulses with incremental delays relative to the incident optical probe pulses (yellow). The incremental spacing is 500ns, or about 0.75mm in depth along the acoustic axis (illustrated schematically in Fig. 4). This represents an initial 1-D image through the sample.

The yellow trace in Figure 6 above is the signal from the gated PMT. A series of pulses can be seen; these are the echo signals from the successive acousto-optic pulse pairs through the sample, as retrieved from the AFC after the carrier pulse has passed through. The incremental relative time delay between acoustic and optical pulses is 500ns, equivalent to a spatial spacing of approximately 0.75mm (on the vertical axis as represented schematically in Fig. 4).

In this manner we are able to track the acoustic pulse through the sample. The relative echo signals provide information on the volume sampled by both light and ultrasound. The results presented here are obtained from a fairly homogeneous phantom with relatively low scattering coefficient. Consequently and as expected, we see an increase in signal as we focus the ultrasound through the center of the optical beam (again, see Figure 4).

Current work is aimed at reconstructing the spatial distribution of material properties based on these signals (imaging) and mapping both scattering and absorbing inclusions embedded in similar gels. In particular, we consider the technique particularly suited for mapping the scattering properties of biological tissue samples. In combination with other techniques (photoacoustic, etc.), we expect to combine these results in a complementary manner to achieve greater imaging quality than is currently possible with either technique alone. We also expect to achieve substantially higher spatial resolution using a higher frequency focusing transducer.

4. CONCLUSIONS

We have developed a quantum memory based technique for the optical detection of ultrasound using cryogenic rare earth ions in a crystalline host, demonstrating record optical sideband to carrier discrimination (49dB). Atomic frequency combs are our quantum memory of choice; we use these to selectively absorb ultrasound modulated sidebands on the carrier light, and retrieve the signals as photon echoes after the carrier pulse has passed through the medium. We demonstrate that the technique remains valid with the use of highly scattered beams as required for the imaging of biological tissues.

We use the described technique to obtain a series of photon echoes from locations evenly distributed along the acoustic propagation axis in a representatively scattering sample. Given the sideband modulation (ultrasound photon ‘tagging’) occurs only from within the acousto-optic common volume, and the modulation depth depends on acoustic and optical intensities and material properties alone, we consider this train of signals representative of an initial 1-D image through the sample. Further optimization is required but already, we note that sub-millimeter resolution can be achieved in the plane perpendicular to the acoustic axis, vertical resolution being limited solely by the operating frequency of the transducer.

Ongoing work is aimed towards further improving discrimination using this technique, and rapidly extending the imaging capabilities to both 2-D and 3-D. In particular, we aim to use the method for spatially mapping the scattering properties of biological tissues, also accounting for absorption on the sample.

We expect the technique to provide high quality images of *in-vivo* biological tissues, and suggest its possible use for early cancer detection.

REFERENCES

[1] Dewhurst, R. J. and Shan, Q., “Optical remote measurement of ultrasound”, Meas. Sci. Technol. 10(11), R139–R168, (1999)

[2] Monchalin, J. P., “Optical detection of ultrasound at a distance using a confocal Fabry-Perot interferometer” Appl. Phys. Lett. 47, 14 (1985)

[3] Ramaz, F., Forget, B. , Atlan, M., Boccara, A. C., Gross, M., Delaye, P. and Roosen, G., “Photorefractive detection of tagged photons in ultrasound modulated optical tomography of thick biological tissues”, Opt. Express 12, 5469 (2004)

[4] Lesaffre, M., Jean, F., Ramaz, F., Boccara, A. C., Gross, M., Delaye, P. and Roosen, G., “In situ monitoring of the photorefractive response time in a self-adaptive wavefront holography setup developed for acousto-optic imaging” Opt. Express 15, 1030 (2007)

[5] Lesaffre, M., Farahi, S., Gross, M., Delaye, P., Boccara, A. C., and Ramaz, F., "Acousto-optical coherence tomography using random phase jumps on ultrasound and light", Opt. Express 17, 18211 (2009)
[6] Bach, T., Jazbinšek, M., Montemezzani, G., Günter, P., Grabar, A. A. and Vysochanskii, Y. M., "Tailoring of infrared photorefractive properties of $Sn_2P_2S_6$ crystals by Te and Sb doping", J. Opt. Soc. Am. B 24, 1535 (2007)
[7] Jazbinšek, M., Haertle, D., Montemezzani, G., Gunter, P., Grabar, A., Stoika, I. and Vysochanskii, Y. M., "Wavelength dependence of visible and near-infrared photorefraction and phase conjugation in $Sn_2P_2S_6$", J. Opt. Soc. Am. B 22, 2459 (2005)
[8] Gross, M., Goy, P., Forget, B. C., Atlan, M., Ramaz, F., Boccara, A. C. and Dunn, A. K., "Time-reversed ultrasonically encoded optical focusing into tissue-mimicking media with thickness up to 70 mean free paths", Opt. Lett. 30, 1357 (2005)
[9] Li, Y., Hemmer, P. R., Kim, C., Zhang, H. and Wang, L. V., "Detection of ultrasound-modulated diffuse photons using spectral-hole burning", Opt. Express 16, 14862 (2008)
[10] Li, Y., Zhang, H., Kim, C., Wagner, K. H., Hemmer, P. R. and Wang, L. V., "Pulsed ultrasound-modulated optical tomography using spectral-hole burning as a narrowband spectral filter", Appl. Phys. Lett. 93, 011111 (2008)
[11] Tay, J. W., Ledingham, P. M. and Longdell, J. J., "Coherent optical ultrasound detection with rare-earth ion dopants", Appl. Opt. 49, 4331 (2010)
[12] Zhang, H., Sabooni, M., Rippe, L., Kim, C., Kroll, S., Wang L. V. and Hemmer, P. R., "Slow light for deep tissue imaging with ultrasound modulation", App. Phys. Lett. 100, 131102 (2012)
[13] McAuslan, D. L., Taylor, L. R. and Longdell J. J., "Using quantum memory techniques for optical detection of ultrasound", Appl. Phys. Lett, 101, 191112 (2012)